Available online at www.sciencedirect.com
SCIENCE DIRECT®
Journal of Microbiological Methods 56 (2004) 173–180
Journal of Microbiological Methods
www.elsevier.com/locate/jmicmeth

Using geographical information techniques to quantify the spatial structure of endolithic boring processes within sediment grains of marine stromatolites

Alexandru I. Petrisor*, Alan W. Decho

Department of Environmental Health Sciences, Arnold School of Public Health, University of South Carolina, Columbia, SC 29208, USA

Received 6 August 2003; received in revised form 28 August 2003; accepted 16 October 2003

Abstract

Marine stromatolites are generated through the interactions of environmental parameters and specific microbial processes. The activities of endolithic bacteria, that bore canals through calcium carbonate ($CaCO_3$) sand grains (ooids) and reprecipitate the $CaCO_3$ as a single layer (i.e. micritic laminae) are especially important in the longer term stability of the stromatolite macrostructure. Image analysis and classification approaches have been used previously, but only seldom as a quantitative microscopic tool. Here, we develop a new approach that enables the quantification of microscale (i.e. micrometers to millimeters) spatial structure within marine stromatolites. To demonstrate our approach, images were acquired from two different layers of a stromatolite: "orange layers", where microboring of canals within ooids was relatively abundant, and "white layers" where microboring was greatly reduced or lacking. Images were then transformed into spatial maps. Computation of canal and ooid grain areas within each image was conducted and statistically compared between replicate samples from the two stromatolite layers. This allowed quantification of the areas of ooid grains that were microbored. Based on our results, we suggest that our method could be widely applicable to sedimentary environments, and other areas of fundamental research.

Keywords: GIS; Confocal; Biofilms; Image analysis; Carbonate; Bacteria

1. Introduction

Marine stromatolites are analogs of the Earth's earliest known mat communities (Reid et al., 2000) and the oldest known macroscopic evidence of life, dating over 3.5 billion years (Visscher et al., 1998). The formation of stromatolites continues in open high-energy marine environments in the Bahamas, and perhaps in other locations. Understanding the activities that lead to their formation may provide insight for early life processes (Grotzinger and Knoll, 1999).

Marine stromatolites are sediment macrostructures having distinct layers (micritic laminae) of precipitated calcium carbonate. The lithification and laminated

* Corresponding author. Tel.: +1-803-777-4144; fax: +1-803-777-3391.
E-mail address: alexandru_petrisor@yahoo.com (A.I. Petrisor).

0167-7012/$ - see front matter © 2003 Elsevier B.V. All rights reserved.
doi:10.1016/j.mimet.2003.10.008

structure is the result of complex interactions of bacteria, sediments and the environment (Reid et al., 2000).

Microscopic analyses show that stromatolite mats consist of four major microbial groups. Cyanobacteria act as primary producers for the system, while aerobic heterotrophs, and sulfate-reducers (SRB) are major heterotrophs, while sulfide-oxidizing bacteria (SOB) can be autotrophs or heterotrophs. The SOB are chemolithotrophic organisms that oxidize reduced sulfur compounds using either O_2 or nitrate as terminal electron acceptors (Jørgensen et al., 1983; Stal et al., 1985; Van Gemerden, 1993; Visscher et al., 1992, 1998). These four bacterial groups cycle through several distinct communities, termed "Type 1, 2, and 3" mats (Reid et al., 2000). The mat types represent a continuum of growth stages (with minimal seasonal variability) and develop sequentially and exhibit increasing microbial complexity. They exhibit different levels of organization and interactions, finally culminating in a close spatial/temporal coupling.

Initially, the surface layer of a stromatolite consists of abundant *Schizothrix*, EPS and ooids (i.e. Type 1 community; Reid et al., 2000). The EPS provides a "sticky" surface for further accretion of ooid grains from the overlying water. This layer grows through accretion of ooids and migrations of *Schizothrix*, and forms a distinct "white layer" with abundant EPS, cyanobacteria and intact ooids. The surface of this white evolves into a nonsticky, lithifying microbial community (Type 2 community), dominated a dense, structured mat of *Schizothrix* sp. and sulfate reducing bacteria (SRB). Concurrent precipitation of a thin (30–50 μm) layer of $CaCO_3$ occurs (Visscher et al., 2001), a process that provides initial stabilization of the underlying ooids and halts further sediment accretion. Finally, ooids, in proximity to the thin precipitate, are colonized by endolithic cyanobacteria (*Solentia* sp.) that microbore and micritize the ooid grains (Type 3 community), ultimately into a solid thick 'micritic' layer of reprecipitated $CaCO_3$ (Reid et al., 2000). The thick micritic layer, resulting from the microboring/precipitation activities of *Solentia* sp., contributes to the longer term physical stabilization (against wave erosion) of the surface of the stromatolite (Reid et al., 2000). A Type I mat then begins on the surface of the stromatolite, to begin a new cycling of microbial communities.

The cycling of communities results in distinct layering within the stromatolites (Reid et al., 2000) having alternating "white layers" containing "intact ooids grains, and "micritized layers" composed of microbored grains (Fig. 1). As a result, some regions of the stromatolite contain ooids that are abundant in microbored canals while in other regions the ooid grains are typically lacking. We used these alternating layers of microbored vs. intact ooids, to develop and demonstrate our optical imaging approach.

Bacterial and biofilm images have been acquired using various microscopy techniques, such as analog techniques (dark-field microscopy, phase-contrast microscopy, interference microscopy, or fluorescence microscopy), and analytical-confocal scanning laser microscopy (CSLM) (Lawrence et al., 1997; Lawrence and Neu, 1999). Images have been processed using various enhancement techniques, such as mathematical filtration, deconvolution, intensity correction, thresholding, cleaning, difference imagery, pseudocolor, contrast stretching, and finally image classification (Lawrence et al., 1997). Previous studies have examined the spatial structure of stromatolites using a confocal scanning laser microscope (CSLM) to analyze samples collected from the Bahamas (Decho and Kawaguchi, 1999; Kawaguchi and Decho, 2000). The $CaCO_3$ (calcite and aragonite) of ooid grains exhibits strong autofluorescence, likely resulting from their unique mineral/organic interaction. Areas of ooid grains that have been modified exhibit dramatically less autofluorescence (488/520 nm; excitation/emission) when examined using CSLM (Fig. 1). This potentially allows discrimination between microbored regions and intact regions of an ooid. These studies have imaged in great detail the alternating layers of a stromatolite to determine which major bacterial species are associated with the layers (Kawaguchi and Decho, 2000). Our previous research has focused on developing a quantitative tool to analyze confocal images using a combined remote sensing and geographical information systems (GIS) approach, transforming confocal images in quantifiable maps (Petrisor et al., 2003).

This research aims to quantitatively analyze images collected from two different types of stromatolite layers, one that containing ooids having abundant microbored canals (i.e. an early Type 3 mat), and a second containing relatively intact ooids (i.e. a Type 1

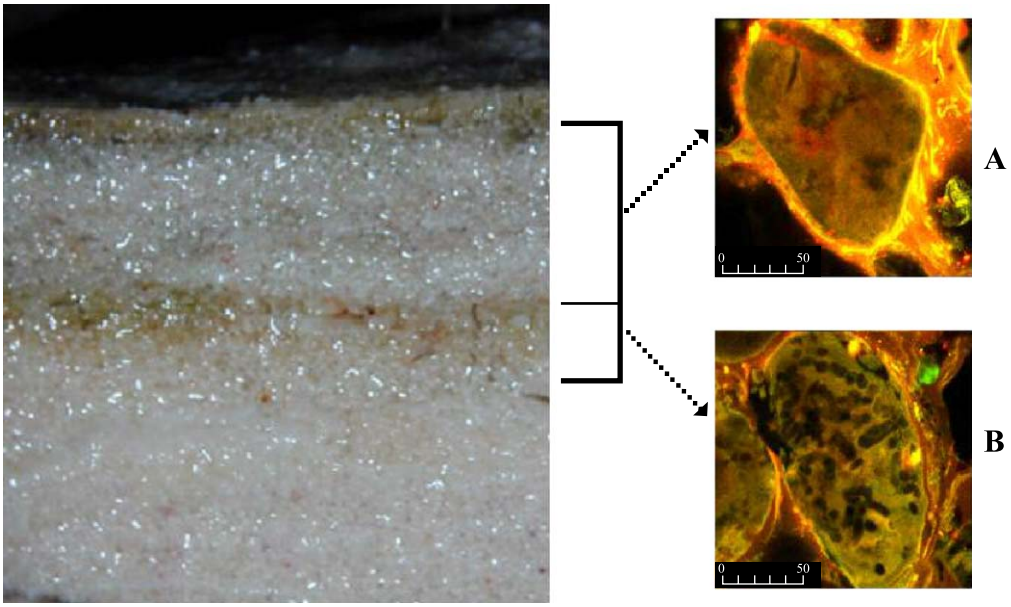

Fig. 1. Showing alternating layers of a typical stromatolite, containing "white layers" of relatively "intact" ooids, and "orange layers" containing intensively microbored/reprecipitated $CaCO_3$. (A) Higher magnification CSLM image showing ooid containing endolithic cyanobacterium *Solentia*, and microbored canals. (B) Higher magnification CSLM image showing relatively 'intact' ooids typically present in white layers.

mat, lacking canals), and provide a quantitative measure of the differences.

2. Materials and methods

All stromatolites, from which samples were collected, came from a subtidal marine environment at Highborne Cay in the Exuma Chain of islands in the Bahamas (76°49′ W; 24°43′ N) (Kawaguchi and Decho, 2000). This site is under current investigation through the Research Initiative on Bahamian Stromatolites (RIBS) project (http://www.home.duq.edu/~stolz/RIBS/index.html). Freshly collected intact stromatolites were sectioned using sterile razor blades. Immediately after collection, the sections of stromatolite were preserved in 3% buffered formaldehyde in seawater. Sections were initially trimmed using a sterile razor, then placed in BEEM embedding molds. Nanoplast® resin (Ted Pella, Redding, CA, USA) and catalyst were thoroughly mixed on site and then added to moulds containing the stromatolites sample. The moulds were placed in a temperature-controlled heat block at 25 °C for 48–60 h to allow slow penetration and complete mixing of the Nanoplast® resin with the hydrated sample. After penetration of the medium, the temperature is raised to 40 °C for 48 h to dry and then 60 °C for 48 h to harden the medium into blocks. The resulting blocks were thick sectioned, mounted on glass microscope slides using Epon 812 and then observed using CSLM (488/520 nm; excitation/emission).

Images were obtained using an MRC 1024MP(7) single and multiphoton system (BioRad Laboratories, Hercules, CA) equipped with a Nikon Eclipse TE 300 compound microscope (Nikon, Tokyo, Japan). Image resolution was 512×512 pixels. For CSLM imaging, three internal detectors were used, each with a six-position emission filter wheel and a variable confocal aperture. Sample slides were viewed using a Nikon Plan Apo 60x objective with immersion oil produced from synthetic hydrocarbons and advanced polymers by Stephens Scientific (catalog #M4004), having a refractive index of 1.515.

Table 1
Explained Arc GIS code to select canals within the ooids in stromatolite images (keywords and commands are in **bold**)

Command	Use of command
w c:\temp	Set work directory, i.e.: c:\temp
Shapearc map_name temp_name_1 **poly**	Save map into Arc GIS format
Clean temp_name_1 **# # 1 poly**	Additional filtering of map
Regionpoly temp_name_1 temp_name_2 **poly** filename.extension	Convert similar regions to polygons
Dissolve temp_name_2 temp_name_3 gridcode	Connect adjacent similar polygons
Reselect temp_name_3 final_name poly	Select features within another feature (canals within ooids)
Res gridcode = ooid_gridcode	Specify that selections should lie within the ooids

Colored composite images were exported in a Bitmap format.

Sixty images each were randomly sampled from two different areas of a stromatolite: (1) an early Type 3 mat, where a developing "orange line" was present and, where ooids contain abundant microboring and canals; and (2) a Type 1 mat or "white layer" area, where ooids were generally intact (i.e. little or no microboring) and canals were largely lacking (Reid et al., 2000). Since the quality of some images was not always suitable for the classification process, the sample size was limited following classification to 30 images from each region.

Each image was classified using supervised classification in Erdas Imagine 8.5. The method allows the user to select sample pixels corresponding to each feature (exopolymer, canals, or ooids) to define specific signatures, and later on the computer performs the classification based on the collection of signatures. Thirty areas have been sampled to define each feature. Following the classification, images were exported into an Arc View GIS 3.X format. Arc View GIS 3.X was used for additional filtering. A 10×10 majority filter produced smoothed, continuous surfaces of all features. The filtered map was saved for the next set of analyses. The resulting maps were analyzed in Arc GIS using the code presented in Table 1.

Significant steps in this process are displayed in Fig. 2 for two images, that are representative for each category ("abundant" canals-1 and "lesser" canals-2): initial image (A), classified image (B), filtered image (C), and reclassified image using the Arc GIS code to select canals within the ooids (D).

The resulting maps were finally analyzed in Arc View GIS to compute the areas of canals and ooids. We propose the following measure for the density of canals:

$$\text{Canal density index(CDI)} = \frac{\text{Area occupied by canals}}{\text{Area occupied by sand grains}} \quad (1)$$

The values of this index range theoretically between 0, if the ooid was entirely intact, and approximately 1, if almost the entire area has been microbored by bacteria. In reality, through the nature of our code, canals communicating with the outside are not selected. Therefore, if all canals communicate with the outside, the index will indicate a value close to 0 instead of approaching 1. This was an additional reason for restricting the sample size. The mean CDIs for the two samples were compared using a *t*-test in SAS® (Cody and Smith, 1997).

3. Results

The results are displayed in Table 2. The *F*-test for the equality of variances indicated that $F = 23.24$ ($p < 0.0001$); therefore, the variances are significantly different and the Satterthwaite method has to be used to look at the differences. In this case, the *t*-value is $t = -6.73$ ($p < 0.0001$); therefore, the mean CDI values are significantly lower in areas with lesser canals.

4. Discussion

Studies by Reid et al. demonstrated that growth of Bahamian stromatolites represented a dynamic bal-

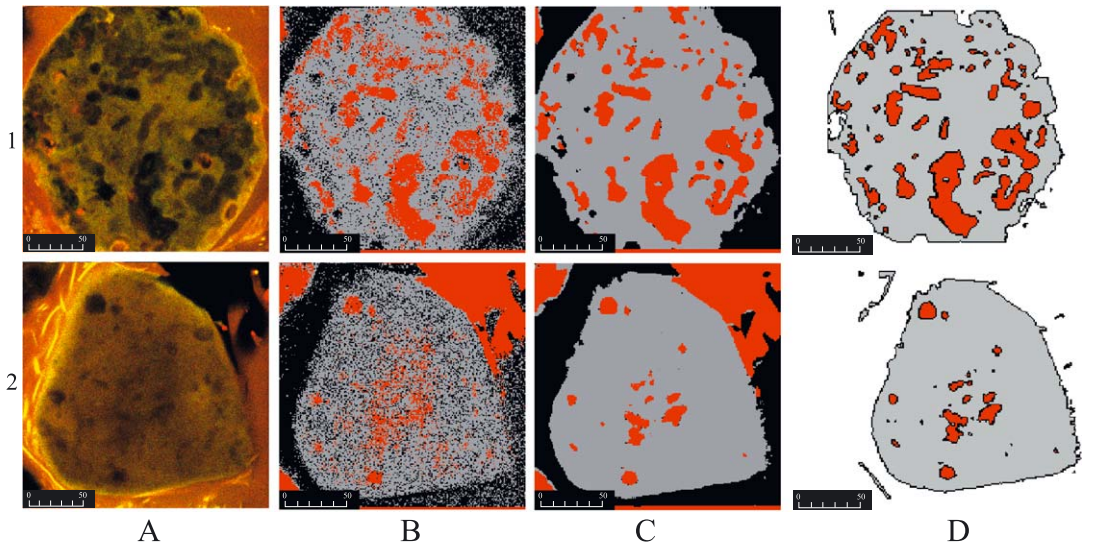

Fig. 2. Illustration of the proposed algorithm using representative images from areas with abundant canals (1) and fewer canals (2). The images display the initial images (A), classified images (B), filtered images (C), and reclassified images with canals selected within the ooids using Arc GIS (D).

ance between sediment accumulation and lithification (Reid et al., 2000). Lithification depends on two fundamentally important microbial processes: photosynthetic production by cyanobacteria, and heterotrophic respiration by bacteria. A laminated microstructure is formed by precipitating laterally continuous sheets of microcrystalline carbonate in surface biofilms at frequent episodic intervals. In some cases, thicker layers of fused grains form below the biofilms in response to microboring activities of coccoid cyanobacteria and precipitation. This micritization of grains contributes to the longer term stability of the stromatolite macrostructure (MacIntyre et al., 2000).

Probing the intact microstructure of sediments is a difficult but important step in understanding how microbial processes influence sedimentary systems. The autofluorescence (488/520 nm; excitation/emission) of natural $CaCO_3$ precipitates allows easy imag-

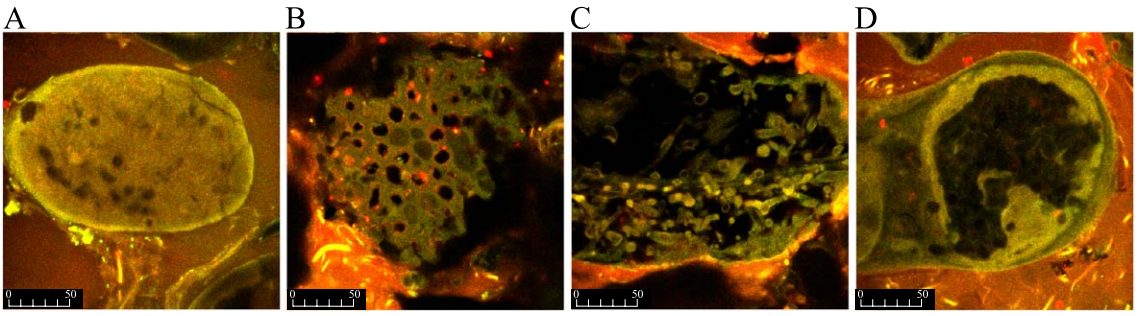

Fig. 3. Sample images from stromatolite (A) "white layers" containing ooids where canals are relatively lacking; (B) a developing "orange line" layers where abundant microboring of ooids has begun, and canals are abundant; (C) a well-developed "orange line" where extensive microboring has occurred and disintegration of ooid into small particles; and (D) the reprecipitation of microbored ooids into a solid "orange line" (i.e. micritic laminae) of $CaCO_3$.

ing of ooid grains using CSLM. This autofluorescence is likely the result of the unique organic-mineral associations of these precipitates. For this reason, the 'canals' within ooids that have been microbored by *Solentia* sp. and filled with new precipitate exhibit considerably less fluorescence and are easily distinguishable from the intact portion of an ooid (Fig. 1B). Thus, CSLM provides an ideal tool for probing the intact structure of sediments.

Microboring by microbial organisms is a common and dynamic process in carbonate environments. A method is described here that when used in conjunction with confocal scanning laser microscopy (CSLM) allows one to quantitatively differentiate the areas of sediment grains (i.e. calcium carbonate ooids) that have been microbored by endolithic cyanobacteria. We analyzed two different areas of the stromatolite that contained either (1) heavily microbored ooids, or (2) relatively intact ooids. The application of our image analysis approach allowed us to differentiate and to quantify the extent of microboring within the ooids from both areas of the stromatolite.

Several points should be noted regarding the classification process. First, supervised classification

Table 2
Results of tabulating areas of ooids and canals within them using Arc View GIS and Arc GIS and computing the canal density index (CDI) for samples taken from regions with abundant canals (A) and lesser canals (B)

Endoliths (A)			Areas with fewer canals (B)		
Ooid Grains	Canals	CDI	Ooid Grains	Canals	CDI
87301.056	17468.111	0.2001	104304.354	9062.860	0.0869
54961.845	9252.470	0.1683	120250.915	14077.982	0.1171
77860.969	57632.042	0.7402	34087.555	310.581	0.0091
82039.317	39371.309	0.4799	99177.219	12937.487	0.1304
89611.039	17971.535	0.2006	104436.733	3614.961	0.0346
72104.001	13026.485	0.1807	72345.044	7647.425	0.1057
121287.308	19032.069	0.1569	67177.177	4617.985	0.0687
89993.324	17938.650	0.1993	185931.192	7163.733	0.0385
63175.782	32243.532	0.5104	170870.552	10529.210	0.0616
126573.537	55110.789	0.4354	109472.221	7713.614	0.0705
74344.277	11632.993	0.1565	113499.593	6949.890	0.0612
95850.927	68079.726	0.7103	116783.607	12565.808	0.1076
69366.343	32284.638	0.4654	151441.409	11516.960	0.0760
155002.433	28876.952	0.1863	106162.750	3956.091	0.0373
80547.170	47695.270	0.5921	153131.785	7576.144	0.0495
126807.841	30233.449	0.2384	95480.794	5768.663	0.0604
99583.350	22258.889	0.2235	195681.404	10758.328	0.0550
62131.690	13647.186	0.2196	198272.975	4709.632	0.0238
155868.645	40152.322	0.2576	170040.638	13487.369	0.0793
130400.504	23796.252	0.1825	68913.377	2270.807	0.0330
92097.951	57055.102	0.6195	214005.692	8930.481	0.0417
119256.672	22489.082	0.1886	92736.479	2464.283	0.0266
88908.126	29411.329	0.3308	95058.200	15249.026	0.1604
90054.983	16445.378	0.1826	183599.288	9434.539	0.0514
123955.086	16142.319	0.1302	135286.098	4684.175	0.0346
131251.398	15813.471	0.1205	158095.993	6919.341	0.0438
93853.176	15176.328	0.1617	127170.256	2403.185	0.0189
122898.662	21724.511	0.1768	110724.729	2897.060	0.0262
101638.649	15538.061	0.1529	131523.483	14021.976	0.1066
119166.239	28568.657	0.2397	124517.587	15523.966	0.1247
		Mean: 0.2936			Mean: 0.0647
		Std. dev.: 0.1825			Std. dev.: 0.0379
		Coeff. var.: 62.2%			Coeff. var.: 58.5%

relies on the ability of the user to identify pixels characteristic to each feature (ooid, exopolymeric matrix etc.). Features like bacteria, ooids or the exopolymeric matrix may be relatively easy to identify and also homogeneous, however, the microbored canals within ooids do not have a unique signature. Also, canals may communicate with the outside of the ooid, or fill with small particulates, remains of bacterial cells, water, and exopolymers. As a result, even if they appear distinct to the naked eye, their resulting spectral signature may not be easily classified, because it is situated at the "intersection" of the signatures belonging to all the other signatures. As a consequence, there is the potential for misclassification, especially where they communicate to the outside or are very close to the outside of the ooid.

Second, there were differences observed between the variances of the two sets of indices (Table 2). However, areas where canals were lacking exhibited high diversity (coefficient of variation = 58.5%). Most of the ooid grains were relatively intact and the variation observed by simply looking at images was very low (Fig. 3A). Meanwhile, in areas where ooids were almost entirely microbored, the calculated variances were different. Since microboring of ooid grains is an ongoing process, this continuum of microboring is reflected in the variance. Some ooids exhibited more canals (Fig. 3B), while some ooids were almost completely torn into pieces due to microboring activities (Fig. 3C). Obviously, images falling into the last category could not be successfully analyzed using our method due to the limitation presented into the methodological section (Fig. 3D).

Nevertheless, our approach provided an analytical tool that enabled us to quantify what has been qualitatively described previously (MacIntyre et al., 2000). We hope that this tool will find applications in fundamental microbiological research and in other areas as well.

Acknowledgements

Authors would like to thank Dr. Tomohiro Kawaguchi from the Department of Environmental Health Sciences for providing the samples, and Wm. Lynn Shirley and Mr. Kevin Remington from the Department of Geography for the Arc GIS code, and the members of the RIBS project (Research Initiative on Bahamian Stromatolites) for helpful discussions. This work was supported by a grant from NSF (EAR-BE 0221796).

References

Cody, R.P., Smith, J.K., 1997. Applied Statistics and the SAS® Programming Language. Prentice Hall, Upper Saddle River, NJ, pp. 138–141.

Decho, A.W., Kawaguchi, T., 1999. Confocal imaging of in situ natural microbial communities and their extracellular polymeric secretions (EPS) using nanoplast resin. BioTechniques 27, 1246–1251.

Grotzinger, J.P., Knoll, A.H., 1999. Stromatolites in Precambrian carbonates: evolutionary mileposts or environmental dipsticks? Annu. Rev. Earth Planet. Sci. 27, 313–358.

Jørgensen, B.B., Revsbech, N.P., Cohen, Y., 1983. Photosynthesis and structure of benthic microbial mats: microelectrode and SEM studies of four cyanobacterial communities. Limnol. Oceanogr. 28, 1075–1093.

Kawaguchi, T., Decho, A.W., 2000. Application of confocal and multi-photon imaging to geomicrobiology. Bio-Rad Application Note 30, pp. 1–6.

Lawrence, J.R., Neu, T.R., 1999. Confocal laser scanning microscopy for analysis of microbial biofilms. Methods Enzymol. 310, 131–144.

Lawrence, J.R., Korber, D.R., Wolfaardt, G.M., Caldwell, D.E., 1997. Analytical imaging and microscopy techniques. In: Hurst, C.J., Knudsen, G.R., Mclnemey, M.J., Stetzenbach, L.D., Walter, M.V. (Eds.), Manual of Environmental Microbiology. Manual of Environmental Microbiology ASM, Washington, pp. 39–61.

MacIntyre, I.G., Prufert-Bebout, L., Reid, R.P., 2000. The role of endolithic cyanobacteria in the formation of lithified laminae in Bahamian stromatolites. Sedimentology 47, 915–921.

Petrisor, A.I., Kawaguchi, T., Decho, A.W., 2003. An introduction to bacterial geography. In: Tepelea, I., Antal, C. (Eds.), Proceedings of the 27th Annual Congress of the American-Romanian Academy of Arts and Sciences, vol. 1. Polytechnic International Press, pp. 158–162.

Reid, R.P., Visscher, P.T., Decho, A.W., Stolz, J., Bebout, B.M., Macintyre, I.G., Paerl, H.W., Pinckney, J.L., Prufert-Bebout, L., Steppe, T.F., DesMarais, D.J., 2000. The role of microbes in the accretion, lamination and early lithification of modern marine stromatolites. Nature 406, 989–992.

Stal, L.J., Van Germerden, H., Krumbein, W.E., 1985. Structure and development of a benthic marine microbial mat. FEMS Microbiol. Ecol. 31, 111–125.

Van Gemerden, H., 1993. Microbial mats: a joint venture. Mar. Geol. 113, 3–25.

Visscher, P.T., Van Ende, F.P., Schaub, B.E.M., Van Gemerden, H., 1992. Competition between anoxygenic phototrophic bacteria

and colorless sulfur bacteria in a microbial mat. FEMS Microbiol. Ecol. 101, 51–58.

Visscher, P.T., Reid, R.P., Bebout, B.M., Hoeft, S.E., Macintyre, I.G., Thompson Jr., J.A., 1998. Formation of lithified micritic laminae in modern marine stromatolites (Bahamas): the role of sulfur cycling. Am. Mineral. 83, 1482–1494.

Visscher, P.T., Reid, R.P., Bebout, B.M., 2001. Microscale observations of sulfate reduction: correlation of microbial activity with lithified micritic laminae in modern marine stromatolites. Geology 28, 919–922.